national accelerator laboratory

FERMILAB-Pub-75/16-THY
ANL-HEP-PR-75-03
January 1975

Isolating the Exchanges in Multiple Production

P. PIRILÄ and G. H. THOMAS
Argonne National Laboratory*, Argonne, Illinois 60439

and

C. QUIGG†
Fermi National Accelerator Laboratory‡, Batavia, Illinois 60510
and
C. C. Lauritsen Laboratory
California Institute of Technology, Pasadena, California 91125

---

*Work performed under the auspices of the U. S. Atomic Energy Commission.

†Alfred P. Sloan Foundation Fellow; also at Enrico Fermi Institute, University of Chicago, Chicago, IL. 60637.

‡Permanent address.

ABSTRACT

We employ rapidity gap distributions to identify and study the exchanges between hadron clusters produced in collisions at Fermilab energies. The observation of charge exchange disproves the neutral cluster model. At these energies, the data are consistent with the independent emission of clusters of limited charge or with a true limited charge-exchange picture. For exchange models, two important parameters are identified: the ratio between $|\Delta Q| = 1$ and $\Delta Q = 0$ exchange, and the ratio between the density in rapidity of charged clusters and that of neutral clusters. In principle, both of these quantities are measurable, but with existing data only the first can be determined. We use a unitarity calculation to estimate the second. Given an exchange model which fits rapidity gap distributions, we obtain a solution to the counting problem in the overlap function calculation of the energy dependence of two-body charge exchange, and estimate the suppression of charge exchange with respect to elastic scattering.

I. INTRODUCTION

In a recent letter[1] we showed that multiparticle production proceeds by the independent emission of multihadron objects (hereafter "clusters") with well-defined average properties which are not strongly dependent upon the total c.m. energy $s^{\frac{1}{2}}$. The experimental evidence on rapidity gap distributions cited there hints that the short-range correlation component which predominates in multiple production is actually generated by an exchange mechanism. Because the same conclusion has consistently been inferred from a large body of circumstantial evidence, it now seems worthwhile to examine other aspects of the exchange picture in respect to the data. The spirit of the present work will be to ask how much information can be established directly from the experimental data. Issues of central concern will be the validity of the exchange picture and the properties of the exchanges.

An immediate abstraction from the exchange picture is the notion of limited charge exchange (LCEX) between the produced clusters. Indeed, the hypothesis of limited charge exchange is precisely the content of the local charge compensation postulate, We shall see that despite assertions to the contrary,[2] the latter can only be formulated in an exchange model. To test the hypothesis, we have examined the rapidity gap length distributions

corresponding to the exchange of fixed charge. An important qualitative result is the observation of charge exchange between clusters. This observation is inconsistent with a literal interpretation of models based on the independent emission of neutral clusters. It should be stressed, however, that past successes of such models in describing and anticipating experimental results have for the most part not rested upon strict neutrality of the clusters. We have found that experimental data at Fermilab energies are in detailed agreement with the hypothesis of limited charge exchange between clusters, but cannot select it uniquely. If the exchange picture is the correct description of particle production, we can determine the properties of the exchanged objects from the data. On this interpretation, charge exchanges -1, 0, + 1 occur with roughly equal frequency. A single important parameter, the ratio of the density in rapidity of charged clusters to that of neutral clusters, cannot yet be measured experimentally.

The information in our possession allows us to implement the program proposed by Krzywicki and Weingarten[2] to bound the separation between the leading Regge intercepts for elastic scattering and two-body charge exchange. We are able to solve the counting problems implicit in their proposal, but our discovery that $\rho_{charged}/\rho_{neutral}$ enters as an independent parameter means that the program as conceived does not lead to a unique result. If in

order to fix the remaining parameter we require the overlap function calculation to yield $\alpha_{CEX} \leq \frac{1}{2}$, we obtain $\rho_{charged}/\rho_{neutral} = 2$.

The body of the article is organized as follows. In Sec. II we first review the direct evidence for independent cluster emission and identify the exchanges between clusters. We then isolate the exchanges of definite charge between clusters, and make qualitative deductions. Two specific interpretations of the data are given in Sec. III: a limited charge exchange model, and a model in which clusters of limited charge are emitted independently. In Sec. IV we review the case for the LCEX model and apply our information to the overlap function estimate of the energy dependence of two-body charge exchange. Summary remarks appear in Sec. V.

II. IDENTIFYING THE EXCHANGES

The independent cluster emission picture satisfactorily describes all the gross features of multiple production at high energies, and many details as well.[3] However, because the average spacing of clusters in rapidity is comparable to the mobility of pions emitted by the clusters, it has been impossible to observe clusters in isolation. Recently we reported[1] direct evidence for the independent emission of clusters in rapidity by proving that (i) the form $P(r) \propto \exp(-\rho r)$ assumed by the rapidity gap distribution for large gap lengths is a direct consequence of independent cluster emission;

(ii) the exponential slope ρ is the density in rapidity of clusters which decay into at least one charged pion; (iii) a deviation from exponential behavior at small separations, in the form of upward curvature, establishes that clusters decay in the mean into more than one charged particle. Although the clusters are not identified individually, we termed this evidence direct because the conclusions follow immediately from the experimental observations, and do not depend upon any fits or Monte Carlo comparisons. In this section, we review and extend the earlier results.

A. Evidence for Independent Cluster Emission

It is assumed in the cluster picture that groups of hadrons are produced independently (therefore according to a Poisson multiplicity distribution) in the available rapidity interval. Each cluster decays isotropically independently of all others, and its decay products are distributed in an uncorrelated manner.

The distribution of gaps between independently emitted objects is

$$P(r) = \rho \exp(-\rho r), \tag{1}$$

where ρ is the density in rapidity of the emitted objects and r is the separation between adjacent objects. If clusters are in fact produced independently, Eq. (1) should describe the unobservable gaps between them. If each cluster is a localized, short-range object

that decays into several hadrons, Eq. (1) is inappropriate for the gaps between particles, because the probability to find short gaps will be enhanced by the propensity of pions from a single cluster to lie near each other in rapidity. However, for gaps so large that the particles on either end must be products of different clusters, Eq. (1) should apply. Thus, we expect to observe the onset of the exponential behavior of (1) when the gap length exceeds the typical range of a cluster (~ 1 unit of rapidity).

Data[4] from pp collisions at three Fermilab energies are displayed in Fig. 1. The rapidity gap distributions for all charged particles[5] show the anticipated behavior: they deviate from a simple exponential at small separations, but the large-gap data are described by exp(-r). The observed large-gap slope implies a cluster density $\rho \approx 1$. This cluster density and the directly-measured charged-pion density[6] $\rho_\pi \approx 2$ suggest that the mean number of charged pions per cluster, $\langle M \rangle$, must be approximately 2. If clusters were neutral, we should therefore expect (1) to hold down to small separations for the gaps between negative particles, since the probability for two negatives to emerge from a single cluster would be exceedingly small. The remaining data in Fig. 1 show this to be the case: the slope for gaps between negatives coincides with the large-gap slope for the all-charged-particles distribution.

To this point we have confirmed directly, on a qualitative level,

that clusters of limited extent in rapidity are produced independently. This conclusion does not rely upon any dynamical assumption concerning the underlying mechanism for particle production, nor do we require any assumption about the intracluster multiplicity distribution to obtain the result $\langle M \rangle \simeq 2$. In Ref. 1 we further showed that the cluster model can quantitatively describe all the data in Fig. 1. The chief ingredient in our subsequent developments will be the idea that the large-gap behavior of the rapidity gap distribution characterizes the exchanges between clusters.

B. Evidence for Charge Exchange

Having determined that the large-gap distribution is characteristic of the spacing between the emitted clusters, we nowattempt to deduce the properties of the exchanges. To do so, we label each rapidity gap by the amount of charge transferred across it. If in an n-charged-particle final state we order the rapidities of the detected particles $y_1 < y_2 < \ldots < y_n$, then the i-th rapidity gap

$$r_i \equiv y_{i+1} - y_i \quad . \quad (2)$$

is said to carry charge

$$\Delta Q_i \equiv \frac{1}{2}\left\{\sum_{k=i+1}^{n} Q(y_k) - \sum_{k=1}^{i} Q(y_k)\right\} , \quad (3)$$

where $Q(y)$ is the charge of the particle detected at rapidity y.

Although we refer to the label ΔQ_i as the charge exchanged across the i-th gap, it can be defined whether or not the secondaries (or the clusters) are actually linked by exchanged particles or Reggeons.

The distributions of gaps which carry $\Delta Q = 0$, $|\Delta Q| = 1$, and $|\Delta Q| \geq 2$ in 205 GeV/c pp collisions are shown in Fig. 2. The shapes of the distributions for $\Delta Q = 0$ and $|\Delta Q| = 1$ are quite similar, and closely resemble the overall distribution of Fig. 1. Both distributions have long tails which extend into the large-gap region that is representative of the gaps between clusters. This observation rules out those models in which strictly neutral hadronic clusters are emitted independently in rapidity, because in such models there can be no charge exchanged between clusters. It is to be emphasized that the many successful predictions of cluster models do not depend upon the simplifying assumption of strict neutrality, but only upon the restriction of cluster charge to low values. There never has been any evidence to support the contention[7] that clusters are "frequently neutral." It is, as we shall see in the next Section, extremely difficult at present energies to fix the relative numbers of produced charged and neutral clusters.

A second qualitative result is the absence of large gaps which carry more than one unit of charge. Such a truncation of the $|\Delta Q| > 1$ distribution is necessary if the exchanges are to be identified with the known mesons. The extent to which this result selects the exchange picture over others is dealt with in Sec. III.

Permitting our observations to become slightly more quantitative, we notice that in the large gap regime, $|\Delta Q| = 1$ gaps are about twice as common as those which carry no charge. At first sight, this is a large ratio which seems inconsistent with folklore based on inclusive cross sections for the exchange of charge between c.m. hemispheres. The latter measure the frequency with which a given amount of charge crosses $y = 0$, irrespective of the length of the central gap. In addition, the largely-diffractive two- and four-prong events exert a strong bias in favor of zero charge transfer. In Fig. 3 we show the charge transfer cross sections for fixed topologies. The higher multiplicities consistently indicate that $\sigma_{\Delta Q = 0}$ is smaller than $\sigma_{|\Delta Q| = 1}$. High multiplicities carry greater weight in the gap distribution than in $\sigma_{\Delta Q}$, where each event is counted only once. There are $n - 1$ gaps in an n-charged particle event. Our procedure is to discard the end gaps from each event, principally to eliminate the very long gaps from diffractive events. This reduces the weight of an n-prong event to n-3. Not all the discarded gaps correspond to Pomeron exchange, but most of them do carry zero charge. Therefore, until the mean multiplicity becomes large, it is difficult to translate the observed ratios of $|\Delta Q| = 1$ gaps to $\Delta Q = 0$ gaps into an accurate measure of the relative strength of the exchanges.

Before going on to the detailed computations of Sec. III, let us summarize our conclusions to this point. We have evidence that at

most one unit of charge is exchanged between clusters in 205 GeV/c pp collisions. Neutral cluster models are eliminated by the observation of charge exchange. In Ref. 1 we noted that because clusters decay on the average into two charged particles, they seem to resemble the low-lying meson resonances. These new results, which imply that clusters carry no more than one unit of charge, heighten the resemblance. Similarly, if an exchange mechanism is responsible for particle production, the exchanges must--like the known resonances--carry limited charge.

III. DETAILED MODELS FOR THE GAP DISTRIBUTIONS

In this section we shall consider two specific interpretations of the gap distributions for charge exchange. The two models have in common the gross features required by the data, notably independent emission with unit density of clusters carrying charge ±1 or 0 which decay into an average of two charged particles. In the first model, the mechanism for independent emission is an explicit exchange scheme, in which a limitation on the charge exchanged between clusters is enforced. This LCEX (limited charge exchange) model is an embodiment of the multiperipheral idea. The alternative description is a model in which explicit exchanges play no role. Equal numbers of positive, negative, and neutral clusters are emitted independently by a mechanism which places no strict limitation on the

amount of charge exchanged across a long gap. In the present energy regime, both descriptions account for all the prominent features of the data. They can be distinguished at higher energies.

For both models, we must specify the intracluster multiplicity distribution. Our previous experience[1] indicates that inclusive gap distributions are insensitive to the form of the distribution, so long as it has the correct mean value. We therefore choose a form which is convenient for computation. The probability g_M for a neutral cluster to decay into M charged particles is

$$g_M = \begin{cases} \beta^M \Big/ I_0(2\beta)\left[\left(\frac{M}{2}\right)!\right]^2, & \text{for M even} \\ 0, & \text{for M odd;} \end{cases} \tag{4}$$

for a singly-charged cluster to decay into M charged particles the probability is

$$g_M = \begin{cases} 0, & \text{for M even} \\ \beta'^M \Big/ I_1(2\beta')\left(\frac{M+1}{2}\right)!\left(\frac{M-1}{2}\right)!, & \text{for M odd .} \end{cases} \tag{5}$$

The parameters β and β' will be adjusted to make the average number of charged pions emitted by all clusters equal to 2. This will guarantee accurate fits to the gap distributions summed over all charge exchanges, but we make no representation that the distributions (4) and (5) are selected by the data.

We shall also assume in both models that the decay of a cluster at rapidity $\hat{y}$ into M particles leads to a distribution

$$D(\hat{y}-y_1)D(\hat{y}-y_2)\cdots D(\hat{y}-y_M) \quad , \tag{6}$$

where

$$D(y) = (2\pi\delta^2)^{-\frac{1}{2}} \exp(-y^2/2\delta^2) \tag{7}$$

and the assumption of isotropic decay requires $\delta \approx 0.85$.

A. A Limited Charge Exchange Model

We have seen in Sec. II that the rapidity gap distributions for specified charge transfer are in qualitative agreement with a simple exchange picture in which the emitted clusters and the exchanges between them carry charges limited to $\pm 1, 0$. At this point we wish to show that such a model can in fact provide an accurate quantitative representation of the data, just as it does[1] if the charge transfers are not distinguished.

It is convenient to label each gap between clusters by the charge transferred across it. We denote the charge carried by the i-th link as e_i. The probability that an n-cluster event will occur with charge exchanges $e_1, e_2 \cdots e_{n+1}$ may be written as

$$P(n|e_1, e_2, \cdots, e_{n+1}) = \frac{(\rho Y)^n}{n!} e^{-\rho Y} g(e_1) \prod_{i=1}^{n} V(e_i|e_{i+1}) g'(e_{n+1}), \tag{8}$$

where $g(e_1)$ is the probability that the beam particle emits a link carrying charge e_1, $V(e_i|e_{i+1})$ is the conditional probability that

a link carrying charge e_i emits a cluster of charge $(e_i - e_{i+1})$ and turns into a link carrying charge e_{i+1}, and $g'(e_{n+1})$ is the conditional probability that a link carrying charge e_{n+1} is accepted by the target particle. The vertex probability can be written in this basis as

$$V(e_i \mid e_{i+1}) = \begin{pmatrix} a_1 & 1-a_1 & 0 \\ \frac{1}{2}(1-a_0) & a_0 & \frac{1}{2}(1-a_0) \\ 0 & 1-a_1 & 1 \end{pmatrix} , \qquad (9)$$

where the rows and columns are labeled as charge 1, 0, -1. Thus, for example, a_0 is the probability that a neutral link emits a neutral cluster and proceeds as a neutral link, whereas $\frac{1}{2}(1-a_0)$ is the probability that a neutral link emits a cluster of charge +1 and proceeds as a negatively-charged link. The zeroes in the extreme off-diagonal elements correspond to the presumed absence of doubly-charged clusters.

The parameters a_0 and a_1 can be related to quantities with direct physical interpretations. The probability that in mid-chain a charged link occurs, emits a charged cluster, and proceeds as a neutral link must be equal to the probability that in mid-chain a neutral link occurs, emits a charged cluster, and proceeds as a charged link:

$$P_{|\Delta Q|=1} \cdot (1-a_1) = P_{\Delta Q=0} \cdot (1-a_0) \quad . \qquad (10)$$

Therefore the ratio of charged exchanges to neutral exchanges is

$$R \equiv P_{|\Delta Q|=1} / P_{\Delta Q=0} = (1-a_0)/(1-a_1) \quad . \qquad (11)$$

The fraction of emitted clusters which are charged can also be read off from Eq. (10). It is

$$\rho_{ch}/\rho = \frac{P_{\Delta Q=0}\cdot(1-a_0)+P_{|\Delta Q|=1}\cdot(1-a_1)}{P_{\Delta Q=0}+P_{|\Delta Q|=1}} = 2\left[1/(1-a_0)+1/(1-a_1)\right]^{-1} . \tag{12}$$

In what follows, we shall often refer to the parameters R and ρ_{ch}/ρ, rather than a_0 and a_1.

We write the end couplings as

$$g(e_1) = (\alpha_1 \quad \alpha_0 \quad \alpha_{-1})$$

and

$$g'(e_{n+1}) = \begin{pmatrix} \alpha'_1 \\ \alpha'_0 \\ \alpha'_{-1} \end{pmatrix} . \tag{13}$$

The symmetry of pp collisions requires that

$$P(n|e_1, e_2, \ldots, e_{n+1}) = P(n|-e_{n+1}, -e_n, \ldots, -e_1) , \tag{14}$$

which is guaranteed by the redefinition

$$g(e_1) = (\mathscr{E}_1 \quad \mathscr{E}_0(2/R)^{\frac{1}{2}} \quad \mathscr{E}_{-1})$$

$$g'(e_{n+1}) = \begin{pmatrix} \mathscr{E}_{-1} \\ \mathscr{E}_0(R/2)^{\frac{1}{2}} \\ \mathscr{E}_1 \end{pmatrix} . \tag{15}$$

A special case will help to explain the origin of conditions (15). Consider the two possible configurations for the reaction

$$p + p \to n + p + (\text{cluster})^{+} \quad ,$$

which are shown in Fig. 4. The first occurs with probability

$$P(1 \mid 0,-1) = \alpha_0 \frac{(1-a_0)}{2} \alpha'_{-1}(\rho Y)e^{-\rho Y} \quad , \tag{16}$$

whereas the second occurs with probability

$$P(1 \mid 1,0) = \alpha_1(1-a_1)\alpha'_0(\rho Y)e^{-\rho Y} \quad . \tag{17}$$

Making the replacement $\alpha_1 = \alpha'_{-1} = \mathscr{E}_1$, which can most simply be deduced from the zero cluster production case, and requiring $P(1 \mid 0,-1) = P(1 \mid 1,0)$, we obtain

$$(1-a_1)\alpha'_0 = \tfrac{1}{2}(1-a_0)\alpha_0 \quad , \tag{18}$$

the connection given implicitly in (15).

To compute the consequences of this model, we sample the distribution (8) by Monte Carlo techniques, and assign each cluster in a generated event a randomly chosen rapidity on the allowed interval $(-Y/2, Y/2)$, where Y is the effective interval occupied by secondaries at the energy in question. In this way we take explicit (but only approximate) account of energy-momentum constraints, without having to make a model for the throughgoing or leading particles. Each cluster decays into a number of charged secondaries sampled from (4) or (5) at rapidities sampled from (6). The observables of interest are built up from the events so generated.

Before comparing the model with the data, it is appropriate to comment on our attitude toward the computations. The important qualitative conclusions of this work were stated in Sec. II. They depend in no way on the numerical results under discussion here. We view the explicit calculations instead as a check on the interpretation of the data given in Sec. II. Therefore we have made no attempt to vary the parameters to achieve cosmetically pleasing fits. On the contrary, we have fixed parameters at the rough values read off from the graphs of the data, where that can be done.

As an example, we show in Fig. 5(a) the predictions of the model, with parameters

$$\rho = 1 \quad , \tag{19}$$

$$\langle M \rangle = 2 \quad , \tag{20}$$

$$R = 2 \quad , \tag{21}$$

deduced from the data and with the values

$$\rho_{ch}/\rho = 2/3 \quad , \tag{22}$$

$$g = (0 \quad 1 \quad 0) \quad , \tag{23}$$

$$g' = \begin{pmatrix} 0 \\ 1 \\ 0 \end{pmatrix} \tag{24}$$

chosen for simplicity, for pp collisions at 205 GeV/c. For our present purposes, the description of the data is quite adequate. The disagreement between model and experiment for $\Delta Q = 0$ may be blamed entirely on

our (too) simple choice for the end couplings. The chosen values of R and ρ_{ch}/ρ correspond to isovector exchanges between isovector clusters, so the requirement that the end links (which we do not count in the plotted distributions) be neutral greatly reduces the probability that low multiplicity (of clusters) events contain neutral links that count. At much higher energies (hence mean multiplicities)the choice of end couplings becomes irrelevant and the model distributions stabilize at the values indicated in Fig. 5(b). The same model is compared with the data from 102 GeV/c and 405 GeV/c pp collisions in Fig. 6. The agreement is quite satisfactory.

Of the seven parameters required to specify the model, three (ρ, $<M>$, and R) have been approximately determined by inspection of the data. The three end couplings are irrelevant at very high energies and could be estimated more closely from other sorts of data. If the decay multiplicity distributions of clusters were known from direct observations, the parameter ρ_{ch}/ρ would be fixed by the requirement that

$$<n(\pi^+)> = <n(\pi^0)> = <n(\pi^-)> \quad . \tag{25}$$

Without such external information, we must ask whether the gap distributions can constrain ρ_{ch}/ρ. We have found that the present data provide no useful constraint. To justify this conclusion, we show in Fig. 7 the results of a 205 GeV/c calculation in which ρ_{ch}/ρ has

been altered grossly, to a value of $\frac{1}{15}$, but other parameters are unchanged. Although the $\Delta Q = 0$ curve is noticeably different from the one in Fig. 5(a), it is not more or less preferred by the data, especially in view of the sensitivity of the curve to the end couplings at this energy. We have not found any direct measure of ρ_{ch}/ρ at even the highest ISR energies.

Even if we cannot fix all the parameters, it may appear that we have verified the correctness of the LCEX picture. However, an alternative model which places no intrinsic limitation on the charge exchanged between clusters also accounts for the data in this energy regime.

B. Independent Emission of Charged Clusters

We now suppose that positive, negative, and neutral clusters are produced with no restriction on the charge (apparently) exchanged between them. On the average, the three species are produced in equal numbers. In each event generated, the number of clusters of each species is sampled from the distribution

$$\frac{\exp(-\rho Y/3)(\rho Y/3)^{n_0+n_{ch}}}{n_0!\left[(n_{ch}/2)!\right]^2 I_0(2\rho Y/3)}\,, \tag{26}$$

where $n_0(n_{ch})$ refers to the number of neutral (charged) clusters. The random assignment of rapidities to the clusters and the subsequent sampling of cluster decays proceeds as in the LCEX model. We shall refer to the present picture as the independent emission of charged clusters (IECC)

model. The prediction of this model at 205 GeV/c are shown in Fig. 5(c) to be in excellent agreement with the data. Therefore, we cannot claim to have any evidence which selects the LCEX picture.

At higher energies, the two models appear much less similar. As the cluster multiplicity increases, the "exchange" of large amounts of charge (e.g., the occurrence of four negative clusters consecutively in rapidity) becomes increasingly likely in the IECC model. Thus, at $Y = 12$ the exchange of two or more units of charge would be nearly as probable as the exchange of no charge [Fig. 5(d)]. The changes are shown more clearly in Figs. 8 and 9. The ratios of the gap distributions for $|\Delta Q| = 1$ and $\Delta Q = 0$ in the two models are shown in Fig. 8 at two energies. These are similar in the two models, tending to the value $R = 2$ at very high energies. In contrast, the ratios of $|\Delta Q| \geq 2$ to $\Delta Q = 0$, shown in Fig. 9, evolve very differently in the models. In the LCEX model, the ratio falls swiftly with increasing gap size, and is (except for the end effects already discussed) essentially independent of energy. In the IECC model, the ratio becomes independent of gap size at infinite energy, and is dramatically increasing as a function of energy in the present regime. On the basis of our Monte Carlo calculations, we feel that an experimental distinction between these alternatives will be possible at energies high in the ISR range.

IV. THE OVERLAP FUNCTION CONNECTION AND THE CASE FOR LIMITED CHARGE EXCHANGE

The recent interest in the overlap function stimulates us to apply what we have learned from the analysis of Fermilab data to the overlap problem. Encouraged by the work of Chan and Paton,[8] Krzywicki and Weingarten and their followers[2] have argued the possibility of computing a bound on the suppression of two-body charge exchange relative to elastic scattering in a model-independent way. The basic assumption is that in certain many-body final states, electric charge is compensated locally in rapidity. The suppression of charge exchange is estimated by means of the unitarity connection between two-body and many-body final states. For forward elastic scattering, one has[9]

$$\begin{aligned} \text{Im } T(ab\to ab) &= \sum_n \langle ab|T|n\rangle\langle n|T|ab\rangle \\ &= \sum_n \sigma(ab\to n) \quad , \end{aligned} \tag{27}$$

whereas for inelastic two-body scattering in the forward direction, the unitarity equation

$$\text{Im } T(ab\to cd) = \sum_n \langle cd|T|n\rangle\langle n|T|ab\rangle \tag{28}$$

contains unknown phases. We may, however, use the Cauchy-Schwartz inequality to replace (28) by

$$|\text{Im } T(ab\to cd)| \le \sum_n \left[\sigma(ab\to n)\,\sigma(cd\to n)\right]^{\frac{1}{2}} \quad . \tag{29}$$

For some time, unitarity-based estimates of the suppression of charge exchange have been made. Ordinarily (in multiperipheral models, for example), ambitious attempts are made to compute the charge exchange amplitude directly, by imposing theoretical prejudices about the phases in (28). The intent of the authors of Ref. 2 was that sufficient data exist (or may soon exist) to compute (27) and (29) without reference to any theoretical model. Instead of relying on models, they proposed to identify the features of the data which control the evaluation of (29).

Krzywicki and Weingarten suggested that local charge compensation is the essential property needed to obtain a suppression from (29). They proposed a formal definition of local compensation which can be tested experimentally. Recently one of us showed that charge has a limited mobility in pp collisions at Fermilab energies.[10] Because local charge compensation is in essence what we have characterized as limited charge exchange, we are in a position to comment directly on the program outlined in Ref. 2.

We showed in Sec. III that at the energies explored the data are equally well described by the LCEX model or the IECC model. The IECC model does not embody local charge compensation, so does not lead to any suppression of the charge exchange cross section. Thus the hope[2] of using data alone to compute the suppression is dashed, at least until higher energy data rule out the IECC description. No model independent

estimate of the suppression can be made at this time.

To proceed any further, we must accept local charge compensation (i.e., LCEX) as a credendum. In formulating the LCEX model, we needed to extract two new parameters from the data: the ratio of $|\Delta Q| = 1$ exchange to $\Delta Q = 0$ exchange between clusters, and the fraction of produced clusters which carry charge. The latter could not be determined from the data but, as we shall show below, the suppression depends sensitively upon it. We are driven to the conclusion that the program of computing the charge exchange suppression directly from the data (even assuming LCEX) cannot yet be realized. To obtain this result we have had to consider how to calculate the suppression in the event of more decisive data. Since our formulation differs from those of earlier authors, we shall now outline our method. The computation is structurally a multiperipheral one,[11] but the calculations in the literature are not executed using clusters, so there are important differences in detail and in interpretation. Because of the structural familiarity of the computation, we will keep our description brief.

To calculate the suppression of charge exchange (CEX) and double charge exchange (DCEX) relative to elastic scattering, we imagine the product $\left[\sigma(ab\to n)\,\sigma(cd\to n)\right]^{\frac{1}{2}}$ to have the form depicted in Fig. 10. The clusters emitted in one process are absorbed in the second, still ordered in rapidity. The end couplings will affect the size of the CEX

cross section, but not the asymptotic power of s which governs the falloff of CEX compared to elastic scattering. (Indeed, the end couplings chosen for the numerical example in Sec. III forbid any CEX.)

Because we are computing only an upper bound on the energy dependence of CEX processes, the square roots of couplings which enter $\left[\sigma(ab\to n)\right]^{\frac{1}{2}}$ must all be taken as positive. The resultant couplings are shown in Fig. 11. The coupling matrix for elastic scattering is

$$G_{EL} = \begin{pmatrix} a_1 & b & 0 \\ b & a_0 & b \\ 0 & b & a_1 \end{pmatrix} , \tag{30}$$

where

$$b = \left[\tfrac{1}{2}(1-a_0)(1-a_1)\right]^{\frac{1}{2}} . \tag{31}$$

The symmetric form of the coupling matrix is related to the probability matrix (9) by a similarity transformation. In the CEX case, the exchanged charges in Fig. 10 must differ by a unit:

$$e_i - e_i' = 1 . \tag{32}$$

There are two independent possibilities, $(e_i, e_i') = (0, -1)$ and $(e_i, e_i') = (1, 0)$, corresponding to a net flow of one unit of charge to the right. The coupling matrix will therefore be

$$G_{CEX} = \begin{pmatrix} (a_0 a_1)^{\frac{1}{2}} & b \\ b & (a_0 a_1)^{\frac{1}{2}} \end{pmatrix} . \tag{33}$$

The only possibility for DCEX is $(e_i, e_i') = (1, -1)$, which implies

$$G_{DCEX} = a_1 \quad . \tag{34}$$

Inserting the coupling matrices into (29), we have

$$|\operatorname{Im} T_{CEX}| \leq e^{-\rho Y} \sum_n (\rho Y G_{CEX})^n / n! \tag{35}$$

and

$$|\operatorname{Im} T_{DCEX}| \leq e^{-\rho Y} \sum_n (\rho Y G_{DCEX})^n / n! \quad , \tag{36}$$

where we are able to carry out the sum over n because we have shown that the clusters may be considered to be emitted independently, with density ρ. The leading asymptotic energy dependences of the CEX and DCEX amplitudes will be given in terms of the (highest) eigenvalues of the coupling matrices. Thus

$$\frac{|\operatorname{Im} T_{CEX}|}{\operatorname{Im} T_{EL}} \leq s^{\rho\left(\lambda_{CEX}^{(+)} - 1\right)} \tag{37}$$

where

$$\lambda_{CEX}^{(\pm)} = (a_0 a_1)^{\frac{1}{2}} \pm b \quad , \tag{38}$$

and

$$\frac{|\operatorname{Im} T_{DCEX}|}{\operatorname{Im} T_{EL}} \leq s^{\rho(a_1 - 1)} \quad . \tag{39}$$

The exponents of s in (37) and (39) bound the energy dependence of CEX and DCEX amplitudes with respect to the elastic amplitude. It

is convenient to write

$$\left.\begin{aligned} \text{Im } T_{EL} &\sim s^{\alpha_{EL}} , \\ |\text{Im } T_{CEX}| &\sim s^{\alpha_{CEX}} , \\ |\text{Im } T_{DCEX}| &\sim s^{\alpha_{DCEX}} , \end{aligned}\right\} \tag{40}$$

where

$$\begin{aligned} \alpha_{EL} - \alpha_{CEX} &\geq \delta_{CEX} , \\ \alpha_{EL} - \alpha_{DCEX} &\geq \delta_{DCEX} . \end{aligned} \tag{41}$$

From (37) and (39), we may read off

$$\begin{aligned} \delta_{CEX} &= \rho - \rho\left[(a_0 a_1)^{\frac{1}{2}} + b\right] \\ &= \rho - \rho\left[\frac{R+1}{2}(2R)^{-\frac{1}{2}} \frac{\rho_{ch}}{\rho} \right. \\ &\quad \left. + \left(1 - \frac{R+1}{2}\frac{\rho_{ch}}{\rho}\right)^{\frac{1}{2}} \left(1 - \frac{R+1}{2R}\frac{\rho_{ch}}{\rho}\right)^{\frac{1}{2}}\right] , \end{aligned} \tag{42}$$

and

$$\begin{aligned} \delta_{DCEX} &= \rho(1-a_1) \\ &= \rho \frac{R+1}{2R} \cdot \frac{\rho_{ch}}{\rho} . \end{aligned} \tag{43}$$

This crude calculation indicates the importance of both R and ρ_{ch}/ρ. In the Appendix, we describe a theoretical calculation of the charge exchange amplitudes (not just bounds) in which isospin properties are imputed to the clusters and the exchanges.

Although the isospin calculation is not in the spirit of the bound-setting program, certain qualitative features do survive. Let us fix R at the approximate value favored by the data, $R = 2$.

The dependence of δ_{CEX} and δ_{DCEX} upon ρ_{ch}/ρ is plotted in Fig. 12, which also contains results for the case $R = 1$. Cf. Fig. 14 for the corresponding (and similar) results in the isospin model. The graph in Fig. 12 shows that it is possible to calculate meaningful bounds on the suppression of charge exchange, once R and ρ_{ch}/ρ are known.

From the discussion of the IECC model above, and from a comparison of Figs. 12 and 14, we conclude that the estimated suppression depends on the calculational scheme and on the values of the physical parameters chosen. We see no hope of making entirely model-independent estimates of δ_{CEX} and δ_{DCEX}. There remains the hope that the suppressions given in (42) and (43) are reasonable and physically useful estimates. By taking them as guides, we can make a very rough estimate of the value of ρ_{ch}/ρ, the parameter we were unable to extract from multiple production data. Choosing $R = 2$ and $\rho = 1$, as suggested by the gap distributions, and identifying the suppression bound with the known charge exchange energy dependence, $\alpha_{CEX} = \frac{1}{2}$, we find that $\rho_{ch}/\rho = \frac{2}{3}$. Other reasonable choices of R and ρ lead in both the isospin scheme and the scheme described above to the suggestion that charged clusters make up a significant fraction of the total. To verify this suggestion directly in the high-energy data would be a noteworthy achievement.

V. SUMMARY

We have shown that multihadron clusters are emitted independently in high energy multiple production. We found that charged exchanges between clusters are quite common, so that literal versions of the neutral cluster picture cannot be correct. The data at Fermilab energies may be explained in terms of either a limited charge exchange model representative of a multiperipheral production mechanism or a model in which charged clusters are emitted independently. At higher energies, these models may be distinguished. If the correct description is the LCEX picture, it is possible to compute, with some model dependence, the suppression of two-body charge exchange compared with elastic scattering. The outstanding failure of this work is our inability to determine from the high-energy data the relative densities of charged and neutral clusters.

In broad perspective, the evidence discussed here seems to us to increase the likelihood that the short-range correlation mechanism in multiparticle production has the properties of an exchange process in which both the exchanged objects and the produced objects resemble the known mesons.

ACKNOWLEDGMENTS

We are grateful to C. Bromberg, R. Engelmann, T. Ferbel, T. Kafka, R. Singer, and J. Van der Velde for communicating their data to us before publication, and to them and the other members of the Argonne/Fermilab/Stony Brook and Michigan/Rochester Collaborations for permission to present their data in this article. One of us (CQ) is indebted to Professor G. C. Fox for his kind hospitality at Cal Tech, where some of the writing was accomplished.

APPENDIX: OVERLAP FUNCTION CALCULATION IN AN ISOSPIN CONSERVING MODEL

In this Appendix we study a simple isospin conserving model for cluster production. We assume that clusters of isospin zero and one are produced by $I = 0$ and $I = 1$ exchanges. Both exchanges are assumed to lead to the same exponential distribution for rapidity gaps between clusters, with the slope of the exponential distribution given by the density of clusters. In standard multiperipheral language, this means that the input singularities are exchange degenerate Regge poles. The model depends upon four independent couplings, which are defined in Fig. 13. In the present calculation we ignore all complex phases out of ignorance, but we retain the signs given by Clebsch-Gordan coefficients.

The matrix element for the production of n clusters with specified charge and isospin is

$$\mathcal{M}_n = \rho^{\frac{1}{2}n} \exp(-\tfrac{1}{2}\rho Y) \sum_{\{I_i\}} \tilde{d}_{I_1,e_1} D^{I_{c1}}_{I_1 e_1, I_2 e_2} D^{I_{c2}}_{I_2 e_2, I_3 e_3} \cdots D^{I_{cn}}_{I_n e_n, I_{n+1}} d_{I_{n+1},e_{n+1}} \quad . \tag{A.1}$$

We denote the isospin of the i-th cluster by I_{ci}, and denote the isospin and charge of the i-th exchange by I_i and e_i. Because we

are interested only in the energy dependence of the overlap function, and not in its magnitude, we need not specify the end couplings $\tilde{d}$ and d. The internal coupling matrix for the production of an isoscalar cluster is

$$D^0 = \begin{pmatrix} \gamma_4 & 0 & 0 & 0 \\ 0 & \gamma_3 & 0 & 0 \\ 0 & 0 & \gamma_3 & 0 \\ 0 & 0 & 0 & \gamma_3 \end{pmatrix}, \qquad (A.2)$$

and for the production of an isovector cluster,

$$D^1 = \begin{pmatrix} 0 & -\gamma_2 & \gamma_2 & -\gamma_2 \\ \gamma_2 & \gamma_1 & -\gamma_1 & 0 \\ \gamma_2 & \gamma_1 & 0 & -\gamma_1 \\ \gamma_2 & 0 & \gamma_1 & -\gamma_1 \end{pmatrix}. \qquad (A.3)$$

Rows and columns of the coupling matrices are labeled by the isospin of the exchanged poles in the order $\phi(I, I_3) = \phi(0,0)$, $\phi(1,-1)$, $\phi(1,0)$, $\phi(1,1)$, where the symbol ϕ denotes a right-moving exchange in Fig. 10.

To determine by means of the optical theorem the positions of all the poles which contribute to forward elastic scattering, we must compute the eigenvalues of the matrix

$$\mathcal{O} = D^{0^+} \otimes D^0 + D^{1^+} \otimes D^1 \quad . \qquad (A.4)$$

The Matrix $\mathcal{O}$ can be reduced to submatrices according to the isospin of the output exchanges. From the decomposition of the isospin product

$$(0 \ominus 1) \otimes (0 \ominus 1) = 0 \oplus 0 \ominus 1 \oplus 1 \ominus 1 \oplus 2 \quad , \qquad \text{(A.5)}$$

we see that there will be two isoscalar poles, three isovector poles, and one isotensor pole. We denote the left-moving exchanges in Fig. 10 by $\bar{\phi}$. A convenient basis for the $I = 0, 1, 2$ submatrices of $\mathcal{O}$ is made up of the objects ψ^I_j :

$$\psi^0_1 = \phi(0,0)\ \bar{\phi}(0,0)$$

$$\psi^0_2 = (3)^{-\frac{1}{2}}\left[\phi(1,1)\ \bar{\phi}(1,1) + \phi(1,0)\ \bar{\phi}(1,0) + \phi(1,-1)\ \bar{\phi}(1,-1)\right]$$

$$\psi^1_1 = (2)^{-\frac{1}{2}}\left[\phi(0,0)\ \bar{\phi}(1,0) - \phi(1,0)\ \bar{\phi}(0,0)\right]$$

$$\psi^1_2 = (2)^{-\frac{1}{2}}\left[\phi(0,0)\ \bar{\phi}(1,0) + \phi(1,0)\ \bar{\phi}(0,0)\right]$$

$$\psi^1_3 = (2)^{-\frac{1}{2}}\left[\phi(1,1)\ \bar{\phi}(1,1) - \phi(1,-1)\ \bar{\phi}(1,-1)\right]$$

$$\psi^2_1 = (6)^{-\frac{1}{2}}\left[-2\phi(1,0)\ \bar{\phi}(1,0) + \phi(1,1)\ \bar{\phi}(1,1) + \phi(1,-1)\ \bar{\phi}(1,-1)\right]$$

In this basis, the neutral isospin eigenstates are coupled through the reduced matrices

$$\mathcal{O}^0 = \begin{pmatrix} \gamma_4^{\,2} & (3)^{\frac{1}{2}}\gamma_2^{\,2} \\ (3)^{\frac{1}{2}}\gamma_2^{\,2} & 2\gamma_1^{\,2} + \gamma_3^{\,2} \end{pmatrix}, \qquad \text{(A.7)}$$

$$\mathcal{O}^1 = \begin{pmatrix} \gamma_3\gamma_4 - \gamma_2^{\,2} & 0 & 0 \\ 0 & \gamma_3\gamma_4 + \gamma_2^{\,2} & 2\gamma_1\gamma_2 \\ 0 & 2\gamma_1\gamma_2 & \gamma_1^{\,2} + \gamma_3^{\,2} \end{pmatrix},$$

(A.8)

$$\mathcal{O}^2 = (\gamma_3^2 - \gamma_1^2) \quad . \tag{A.9}$$

The requirement that the highest isoscalar eigenvalue be unity leads to the condition

$$3\gamma_2^4 = (1-2\gamma_1^2 - \gamma_3^2)(1-\gamma_4^2) \quad . \tag{A.10}$$

Then the eigenvalues λ_j^I corresponding to the output intercepts are

$$\begin{aligned}
\lambda_1^0 &\equiv 1 \\
\lambda_2^0 &= 2\gamma_1^2 + \gamma_3^2 + \gamma_4^2 - 1 \\
\lambda_{1,2}^1 &= \frac{\gamma_1^2 + \gamma_2^2 + \gamma_3^2 + \gamma_3\gamma_4}{2} \pm \left[\left(\frac{\gamma_1^2 - \gamma_2^2 + \gamma_3^2 - \gamma_3\gamma_4}{2}\right)^2 + 4\gamma_1^2\gamma_2^2\right]^{\frac{1}{2}} \\
\lambda_3^1 &= \gamma_3\gamma_4 - \gamma_2^2 \\
\lambda_1^2 &= \gamma_3^2 - \gamma_1^2
\end{aligned} \tag{A.11}$$

The same isovector and isotensor intercepts can be obtained by studying the forward charge exchange overlap, and the isotensor intercept occurs again in the double charge exchange overlap function.

To compare this model with the computation described in Sec. IV, we express the quantities R and ρ_{ch}/ρ in terms of the present parameters. The relations are

$$R = 2/(1+3R_I) \quad , \tag{A.12}$$

and

$$\rho_{ch}/\rho = \frac{4}{3}\,\frac{(1-\gamma_1^2-\gamma_3^2)}{1+R_I} \quad , \tag{A.13}$$

where

$$R_I = (1-2\gamma_1^2-\gamma_3^2)/(1-\gamma_4^2) \qquad (A.14)$$

is the asymptotic ratio of isoscalar to isovector exchange. We observe that having chosen ρ, R, ρ_{ch}/ρ and enforced (A.10), we are left with one additional free parameter, which reflects the possibility of correlations between successive exchanges which were absent in the simpler model discussed in the text.

According to a well-known result for multiperipheral models, the output intercepts are given in terms of the input α_{in} by

$$\alpha = 2\alpha_{in} - 1 + \rho\lambda \quad . \qquad (A.15)$$

A constant total cross section is generated by

$$\alpha_{in} = 1 - \tfrac{1}{2}\rho \quad , \qquad (A.16)$$

which leads to

$$\alpha = 1 - \rho(1 - \lambda) \quad . \qquad (A.17)$$

Independently of an auspicious choice for α_{in}, the splitting between the leading isoscalar intercept and those for the highest-lying isovector and isotensor trajectories are given by

$$\delta\,(I=1) = \delta\,(CEX) = \rho(\lambda_1^0 - \lambda_1^1) \quad , \qquad (A.18)$$

$$\delta\,(I=2) = \delta\,(DCEX) = \rho(\lambda_1^0 - \lambda_1^2) \quad . \qquad (A.19)$$

In Fig. 14 we show δ (I=1) and δ (I=2) as functions of ρ_{ch}/ρ for $\rho = 1$ and R= 2 or 1. That the separations are not uniquely determined for $R \neq 2$ is due to the additional free parameter in this model.

FOOTNOTES AND REFERENCES

[1] C. Quigg, P. Pirilä, and G. H. Thomas, Phys. Rev. Letters 34, (1974).

[2] A. Krzywicki and D. Weingarten, Phys. Letters 50B, 265 (1974); P. Grassberger, C. Michael, and H. I. Miettinen, Phys. Letters 52B, 60 (1974).

[3] A. W. Chao and C. Quigg, Phys. Rev. D9, 2016 (1974); S. Pokorski and L. Van Hove, Acta Phys. Polon. B5, 229 (1974); G. H. Thomas, Proc. XVII Int. Conf. on High Energy Physics, ed. J. R. Smith (Chilton: Rutherford Lab, 1974), p. I-83.

[4] Argonne/Fermilab/Stony Brook Collaboration, to be published (205 GeV/c data); Michigan/Rochester Collaboration, to be published (102 and 400 GeV/c data).

[5] End gaps have been eliminated to minimize distortions due to diffractive events.

[6] J. Whitmore, Phys. Reports 10C, 273 (1974).

[7] L. Van Hove, CERN Courier 14, 331 (1974).

[8] Chan Hong-Mo and J. E. Paton, Phys. Letters 46B, 228 (1973).

[9] We omit irrelevant kinematical factors from the following equations, which may be regarded as schematic.

[10] C. Quigg, FERMILAB-Pub-74/104-THY.

[11] See, e.g. D. R. Snider and P. W. Coulter, Phys. Rev. D8, 4055 (1973), and citations therein.

FIGURE CAPTIONS

Fig. 1 Distribution of rapidity gaps between produced particles in pp collisions at Fermilab energies (from Ref. 4).

Fig. 2 Distribution of rapidity gaps carrying specified charge in 205 GeV/c pp collisions (from Ref. 4).

Fig. 3 Charge transfer cross sections as a function of event topology in 205 GeV/c pp collisions.

Fig. 4 Two configurations for the reaction $p+p \to n+p+(\text{cluster})^+$.

Fig. 5 (a) Comparison of a simple limited charge exchange model with the 205 GeV/c gap distributions.
(b) The LCEX model at a much higher energy.
(c) Comparison of the independent emission of charged clusters model with the 205 GeV/c data.
(d) The IECC model at a much higher energy.

Fig. 6 Comparison of the LCEX model with (a) 102 GeV/c data; (b) 400 GeV/c data.

Fig. 7 A LCEX model with $\rho_{ch}/\rho = 1/15$, compared with the 205 GeV/c data.

Fig. 8 Ratio of charge 1 to charge 0 exchange (a) in the LCEX model at 205 GeV/c; (b) at a much higher energy; (c) in the IECC model at 205 GeV/c; (d) at a much higher energy.

Fig. 9 Similar to Fig. 8 for the ratio of charge 2 exchange to charge 0 exchange.

Fig. 10 The structure of the overlap function in the LCEX picture.

Fig. 11 The independent couplings which occur in Fig. 10, for the charge basis model described in the text.

Fig. 12 Bounds on the separations between the leading elastic and charge exchange intercepts and between the leading elastic and double charge exchange intercepts computed in the charge basis model.

Fig. 13 Independent couplings which occur in Fig. 10, for the isospin basis model described in the Appendix.

Fig. 14 The separations $\delta(I=1)$ and $\delta(I=2)$ computed in the isospin model.

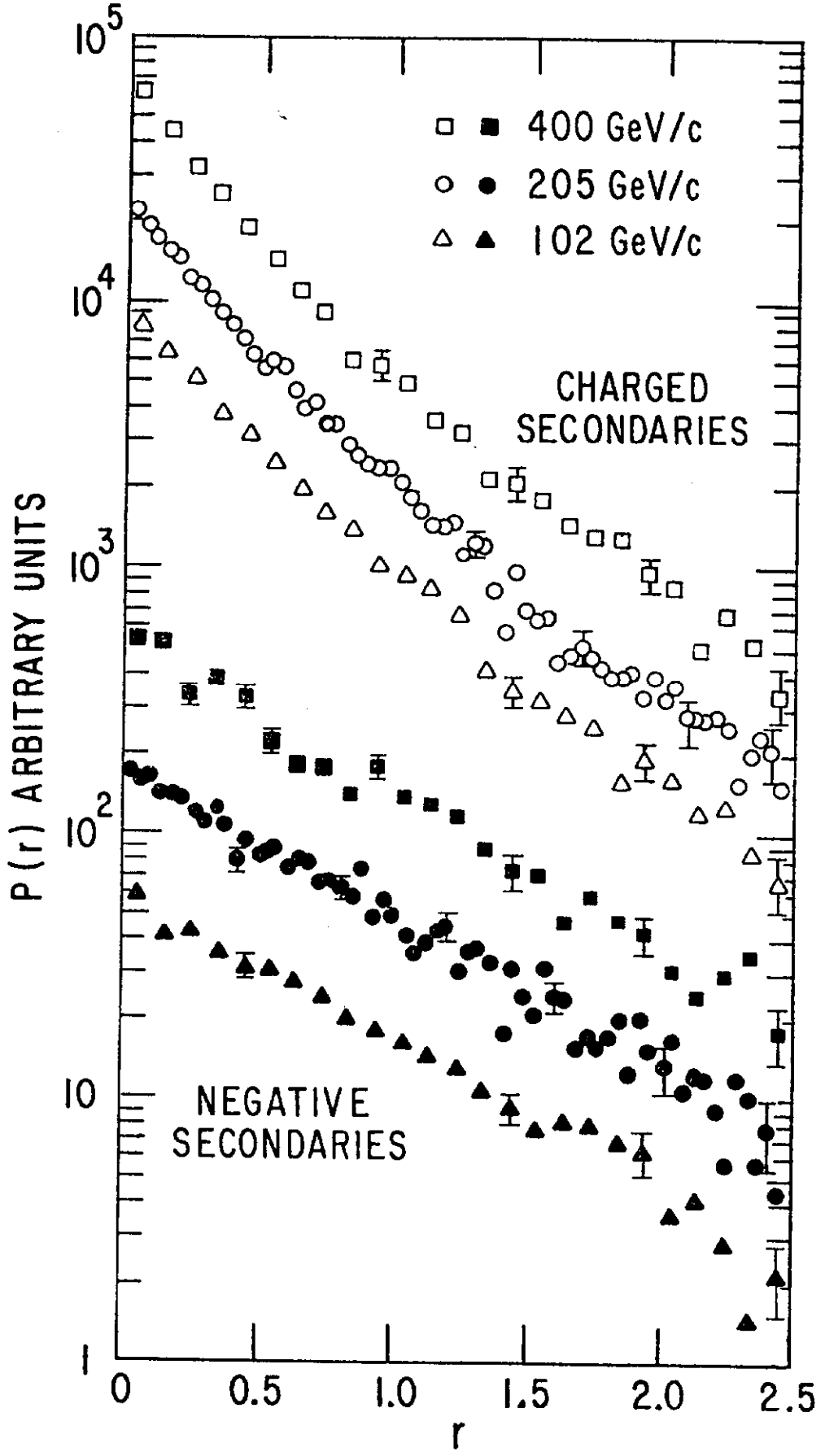
400 GeV/c
205 GeV/c
102 GeV/c
CHARGED SECONDARIES
NEGATIVE SECONDARIES
P(r) ARBITRARY UNITS
r
10^5
10^4
10^3
10^2
10
1
0
0.5
1.0
1.5
2.0
2.5

Fig. 1

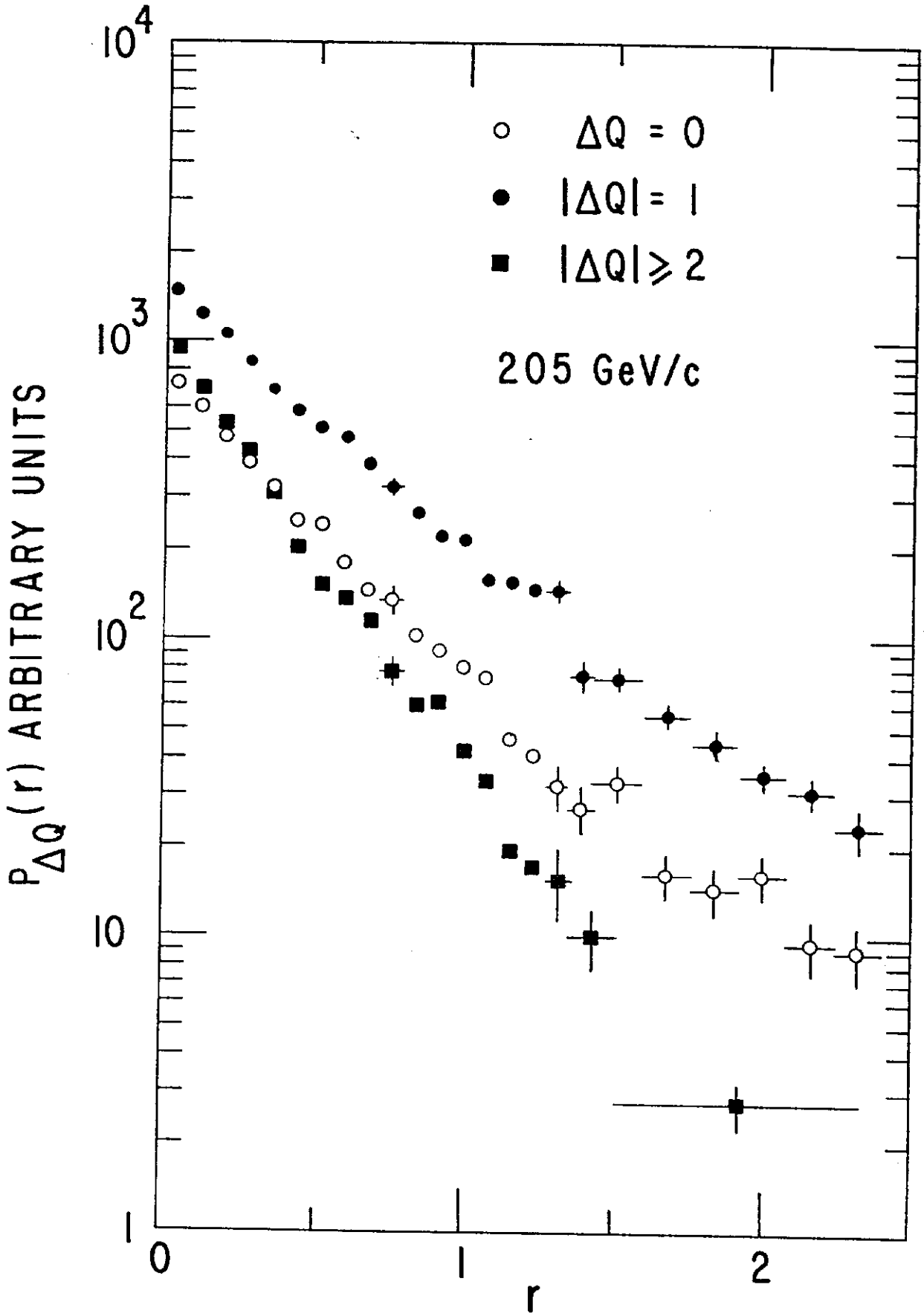
10^4
10^3
10^2
10
1
0
1
2
r
$P_{\Delta Q}(r)$ ARBITRARY UNITS
$\Delta Q = 0$
$|\Delta Q| = 1$
$|\Delta Q| \geq 2$
205 GeV/c

Fig. 2

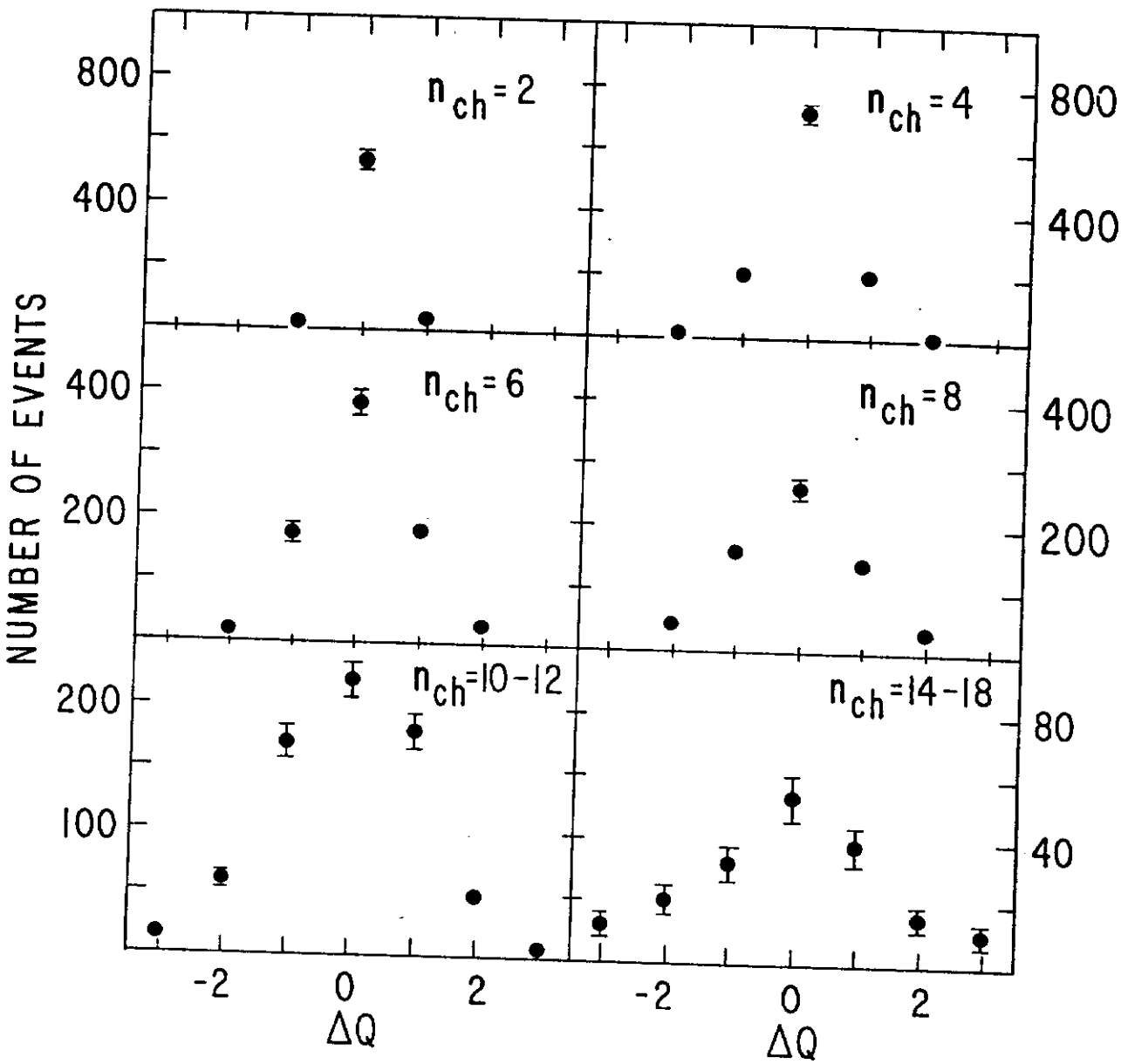
NUMBER OF EVENTS
800
400
400
200
200
100
800
400
400
200
80
40
$n_{ch}=2$
$n_{ch}=4$
$n_{ch}=6$
$n_{ch}=8$
$n_{ch}=10-12$
$n_{ch}=14-18$
-2
0
2
ΔQ
-2
0
2
ΔQ

Fig. 3

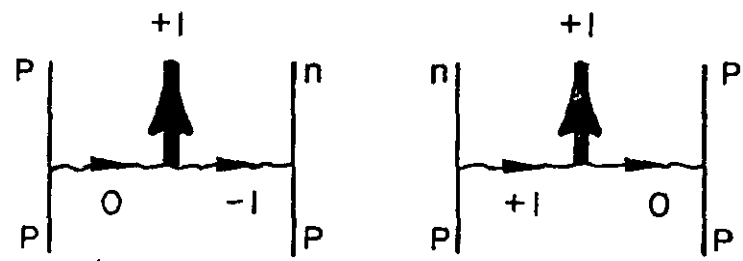

Fig. 4

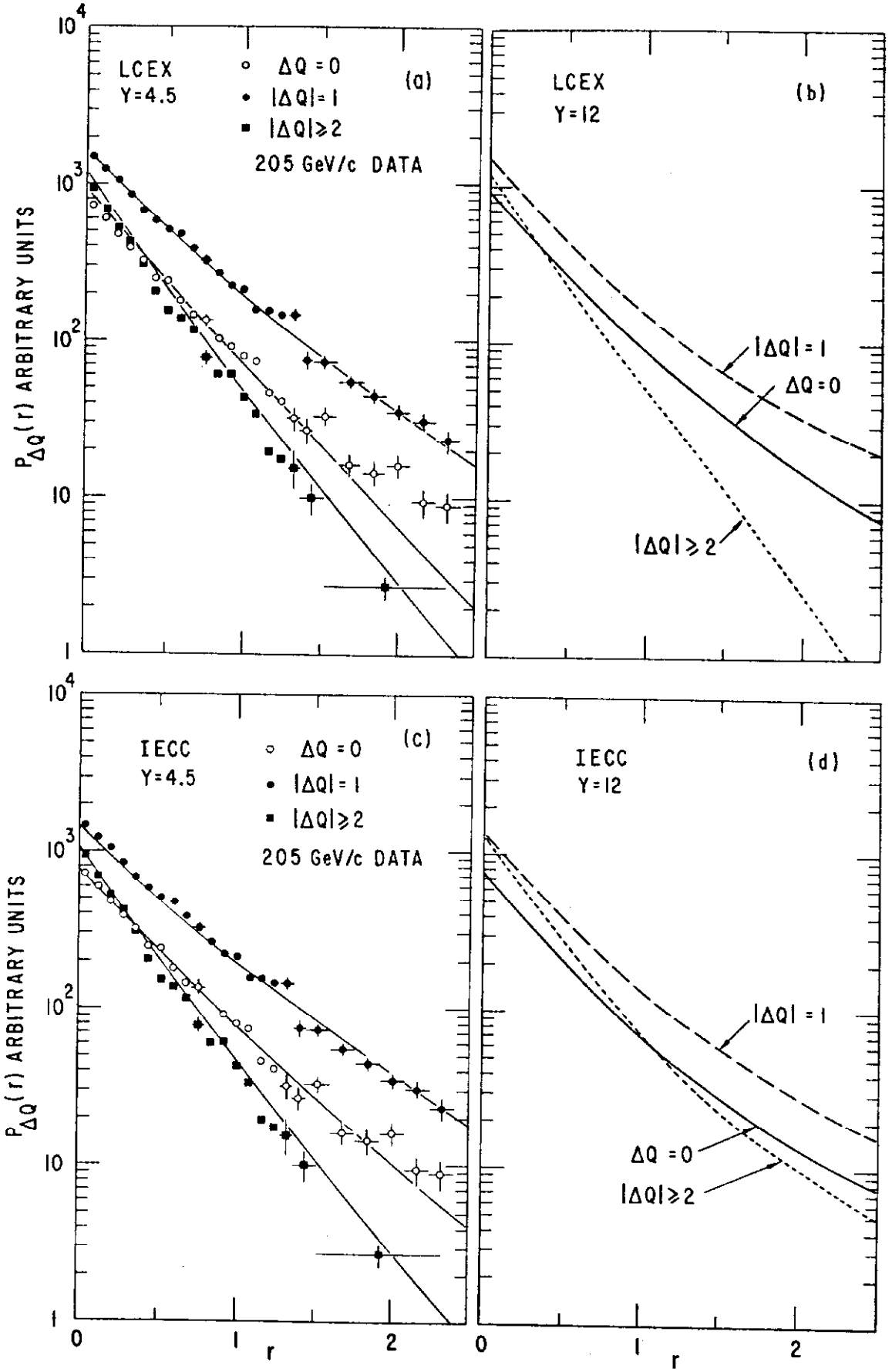
LCEX
Y=4.5
ΔQ = 0
|ΔQ| = 1
|ΔQ|≥2
205 GeV/c DATA
(a)
LCEX
Y=12
(b)
|ΔQ| = 1
ΔQ = 0
|ΔQ|≥2
IECC
Y=4.5
(c)
IECC
Y=12
(d)
$P_{\Delta Q}(r)$ ARBITRARY UNITS
r

Fig. 5

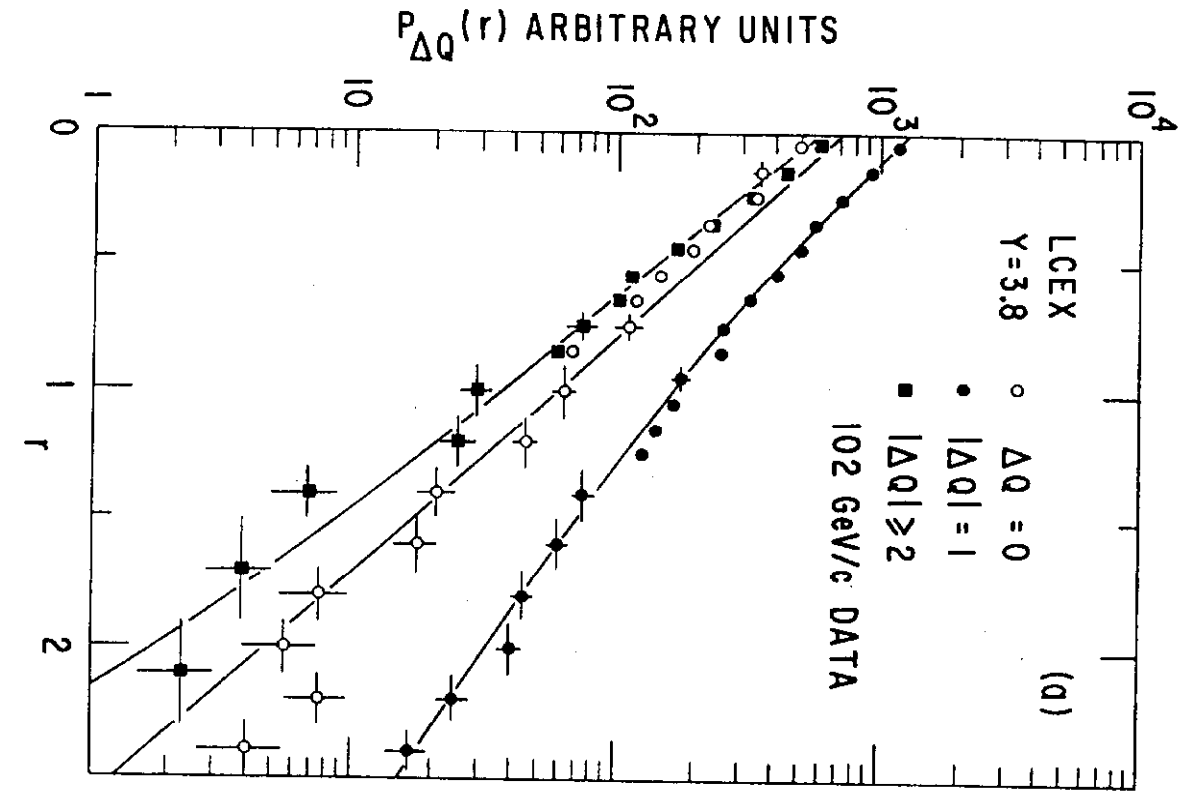
$P_{\Delta Q}(r)$ ARBITRARY UNITS
1
10
10^2
10^3
10^4
0
1
2
r
LCEX
Y=3.8
○ ΔQ = 0
● |ΔQ| = 1
■ |ΔQ|≥2
102 GeV/c DATA
(a)

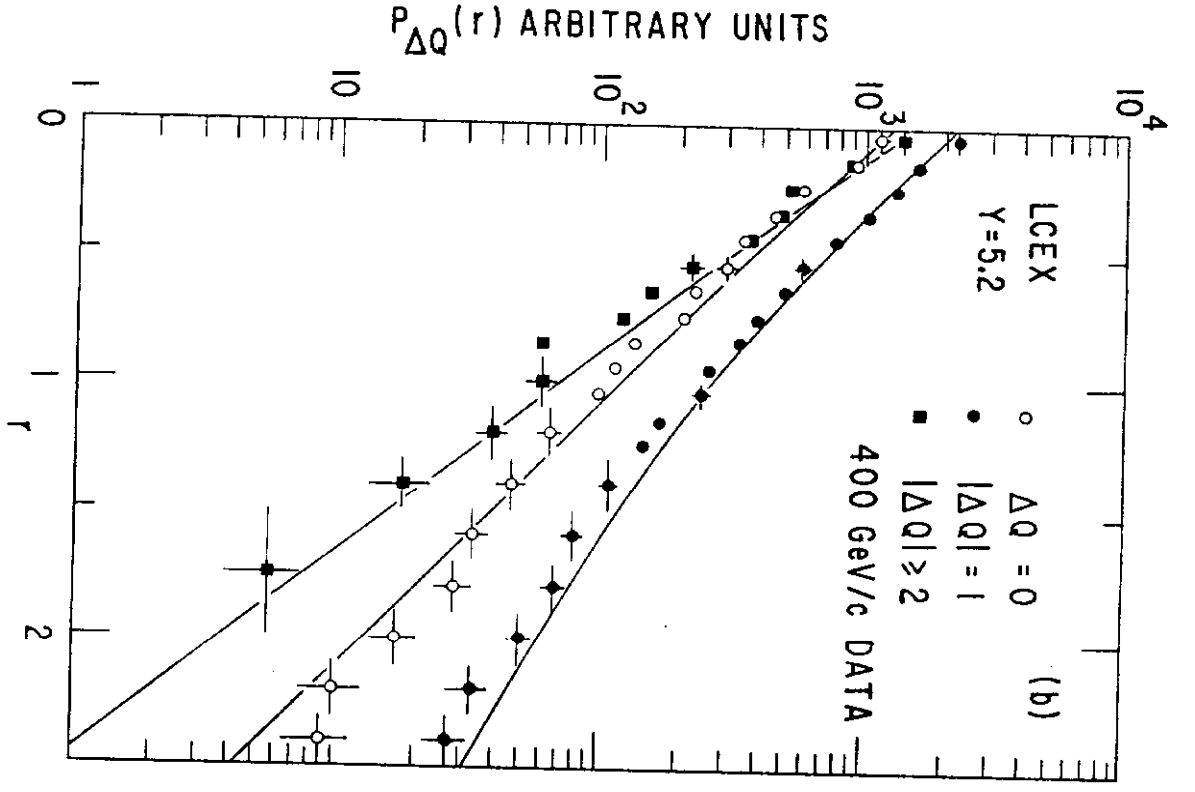
$P_{\Delta Q}(r)$ ARBITRARY UNITS
1
10
10^2
10^3
10^4
0
1
2
r
LCEX
Y=5.2
○ ΔQ = 0
● |ΔQ| = 1
■ |ΔQ|≥2
400 GeV/c DATA
(b)

Fig. 6

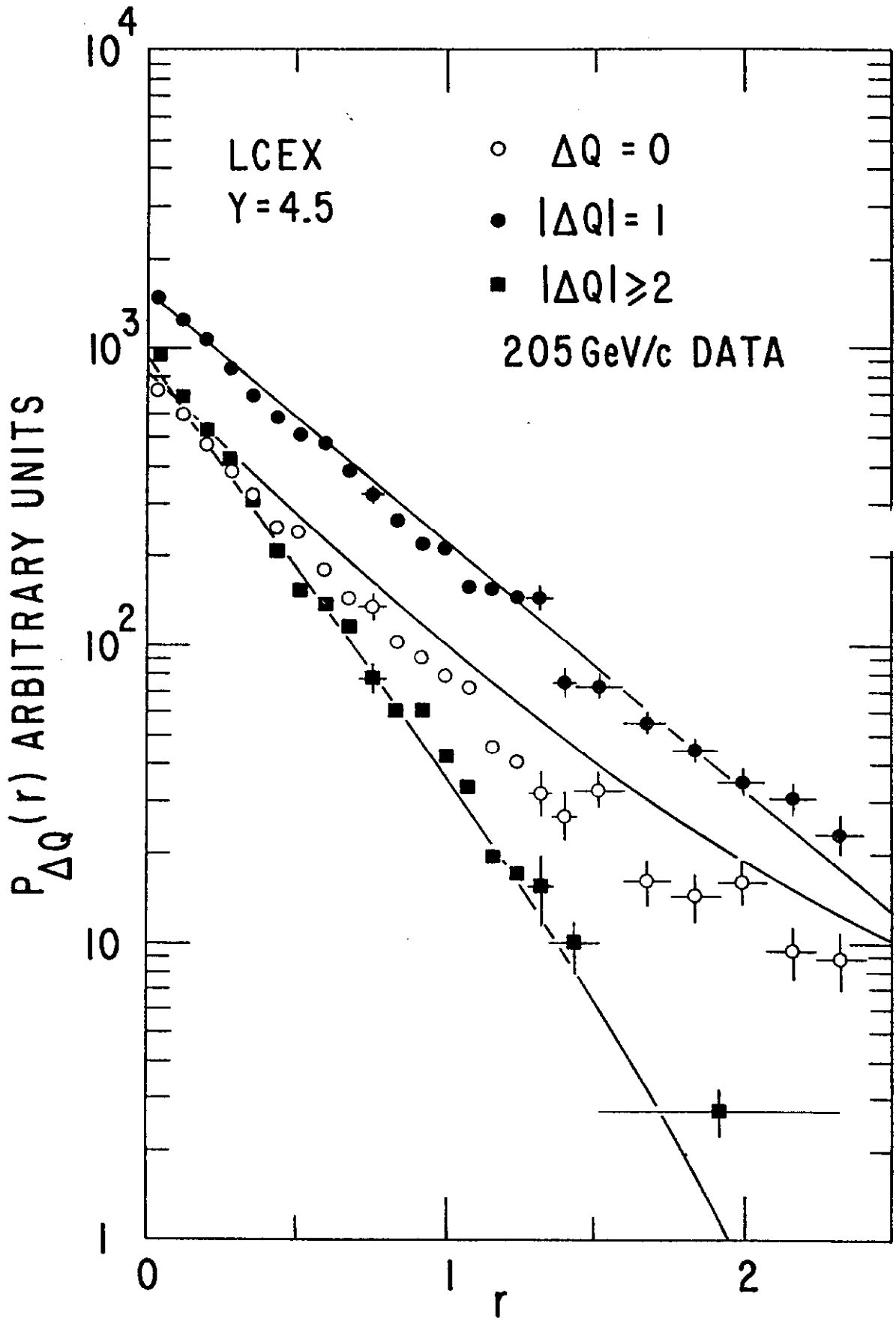
LCEX
Y = 4.5
ΔQ = 0
|ΔQ| = 1
|ΔQ| ≥ 2
205 GeV/c DATA
$P_{\Delta Q}(r)$ ARBITRARY UNITS
10^4
10^3
10^2
10
1
0
1
2
r

Fig. 7

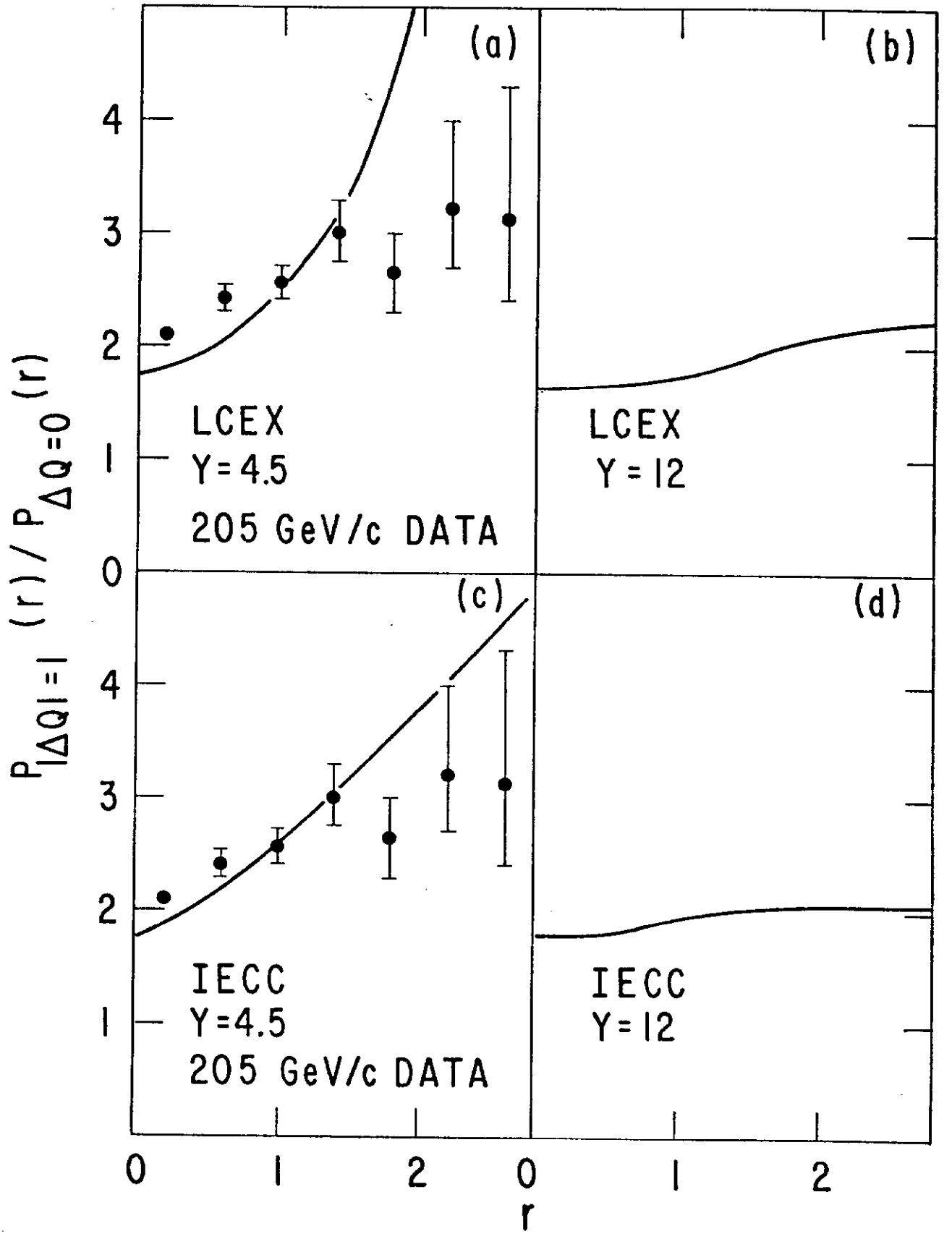
(a)
(b)
(c)
(d)
LCEX
Y = 4.5
205 GeV/c DATA
LCEX
Y = 12
IECC
Y = 4.5
205 GeV/c DATA
IECC
Y = 12
$P_{|\Delta Q|=1}(r) / P_{\Delta Q=0}(r)$
r
0
1
2
3
4

Fig. 8

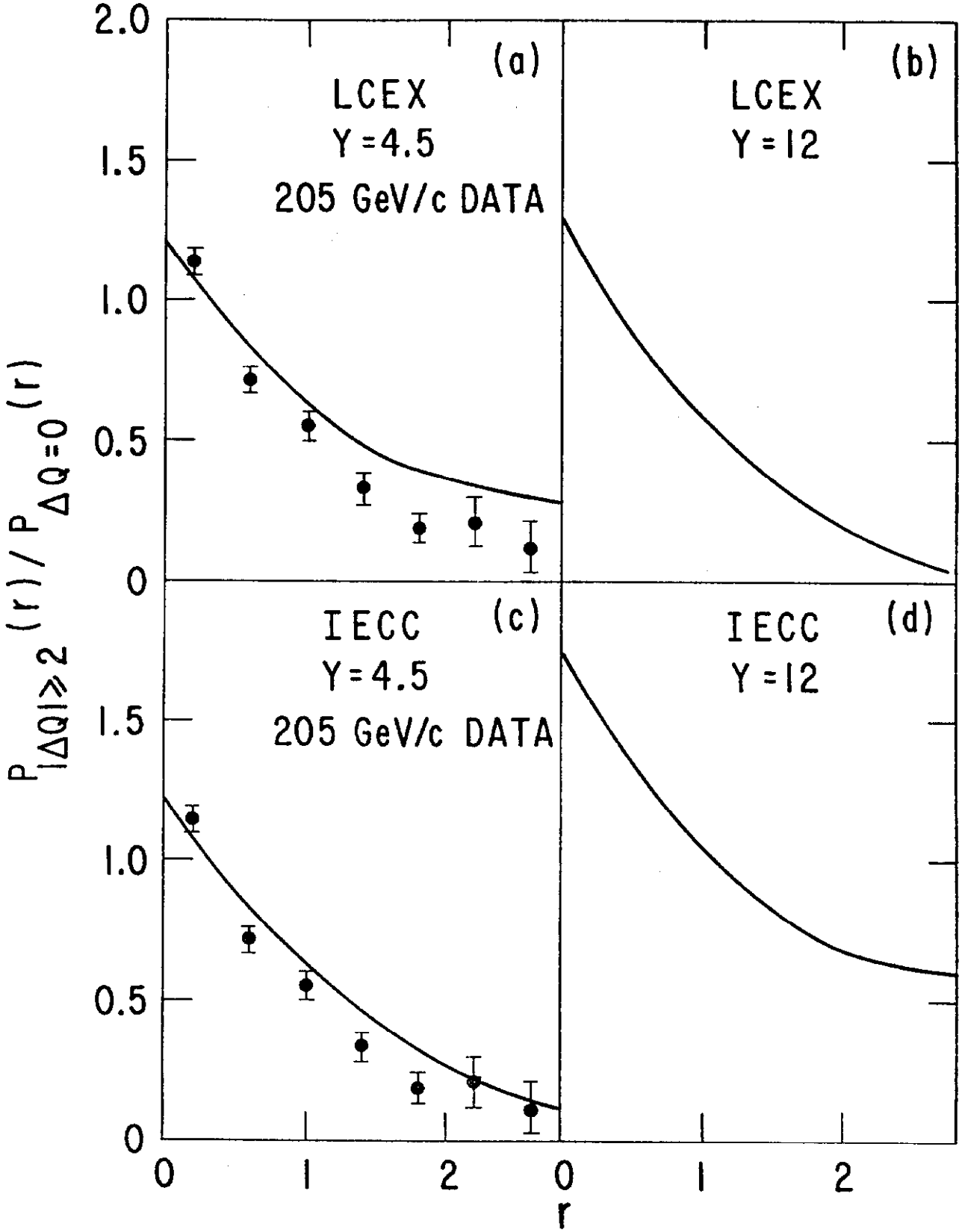
(a)
LCEX
Y=4.5
205 GeV/c DATA
(b)
LCEX
Y=12
(c)
IECC
Y=4.5
205 GeV/c DATA
(d)
IECC
Y=12
$P_{|\Delta Q|\geq 2}(r) / P_{\Delta Q=0}(r)$
r
0
0.5
1.0
1.5
2.0
1
2

Fig. 9

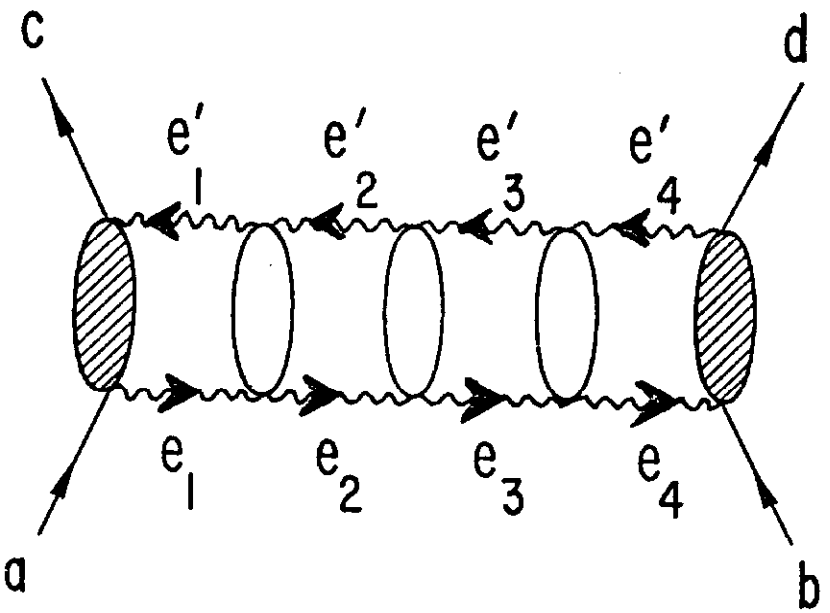

Fig. 10

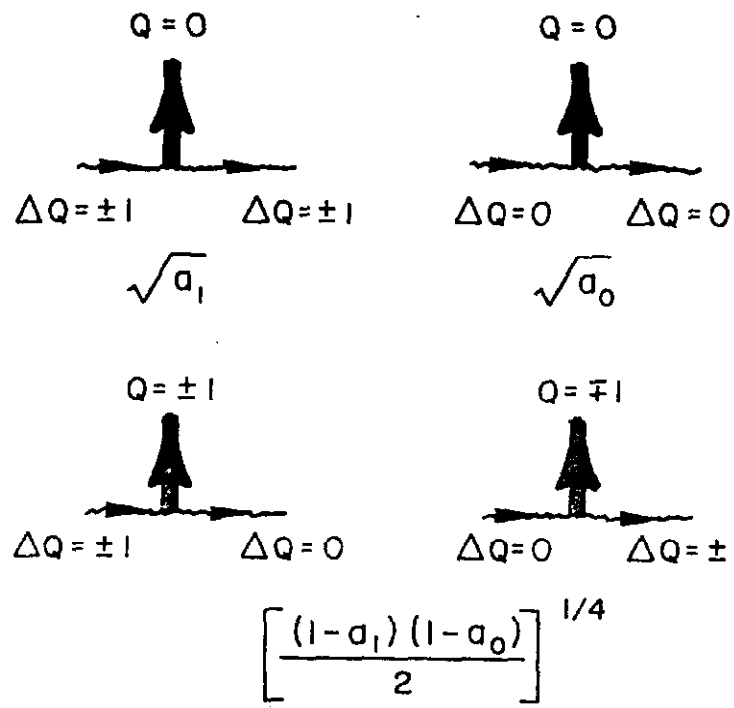

Fig. 11

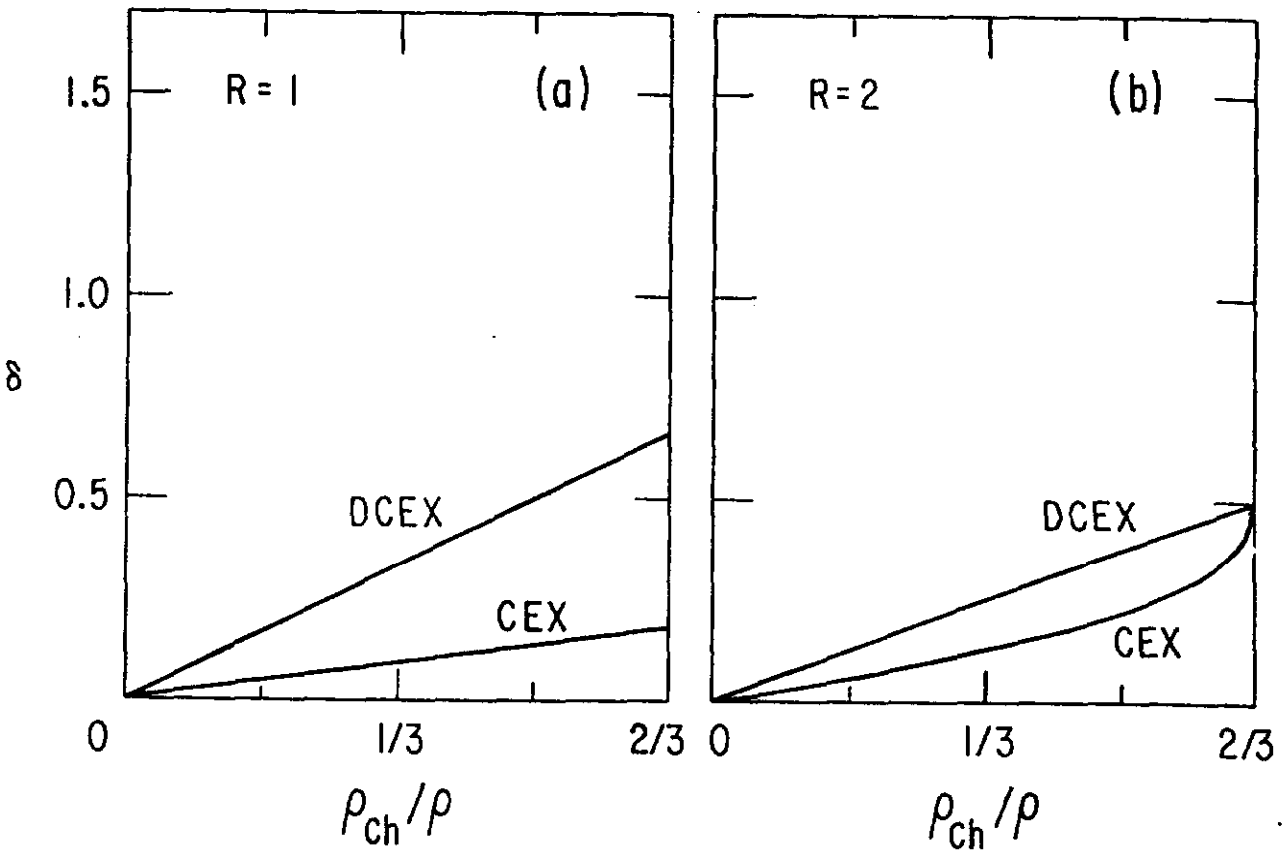
1.5
1.0
0.5
0
δ
R = 1
(a)
DCEX
CEX
1/3
2/3
ρ_{Ch}/ρ
R = 2
(b)
DCEX
CEX
0
1/3
2/3
ρ_{Ch}/ρ

Fig. 12

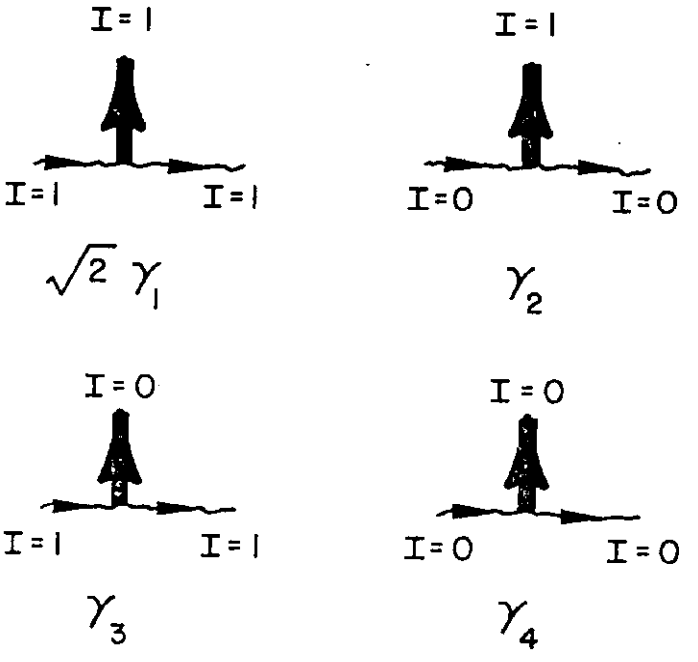
I=1
I=1
I=1
$\sqrt{2}\,\gamma_1$
I=1
I=0
I=0
γ_2
I=0
I=1
I=1
γ_3
I=0
I=0
I=0
γ_4

Fig. 13

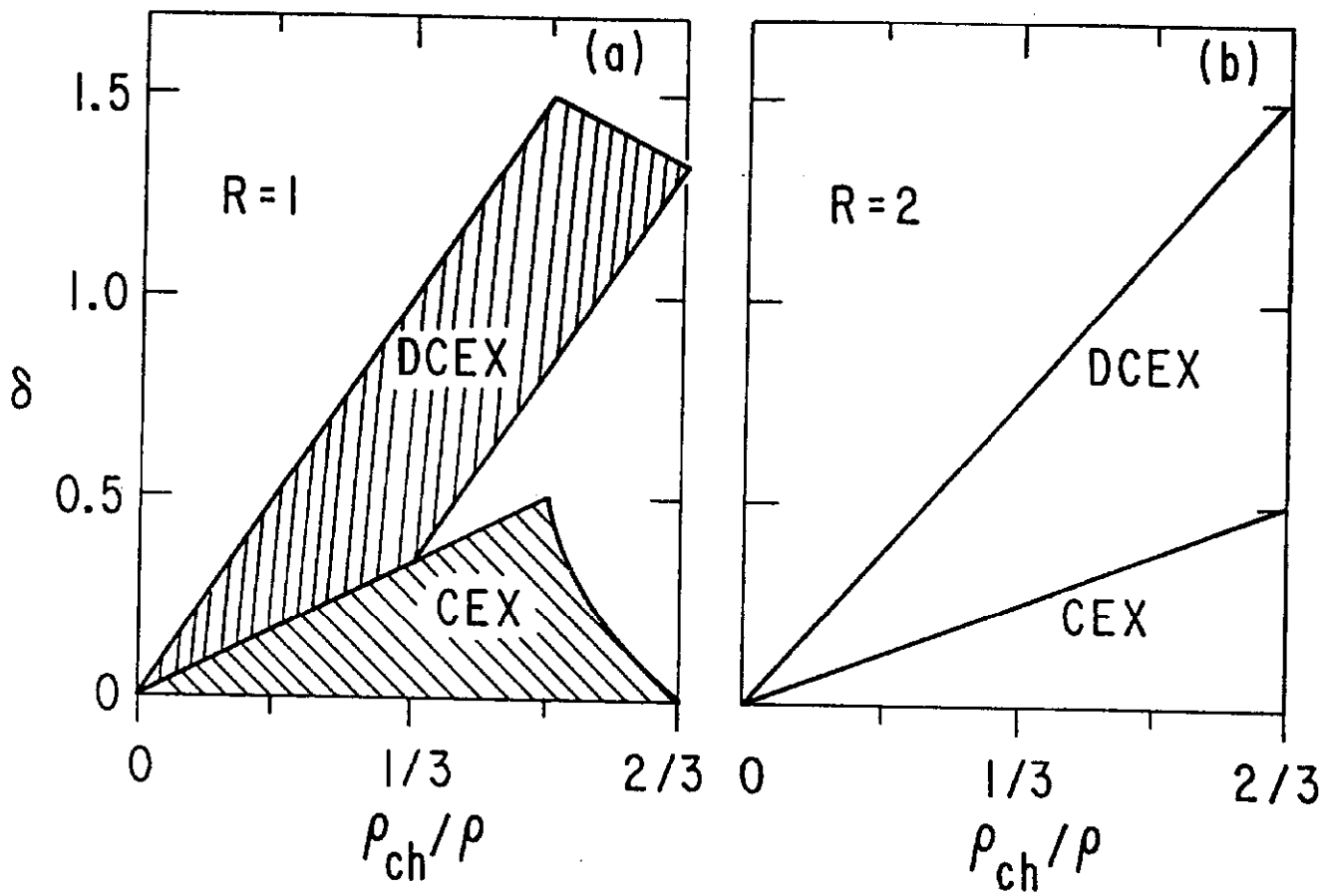
(a)
R = 1
DCEX
CEX
1.5
1.0
0.5
0
δ
0
1/3
2/3
ρ_{ch}/ρ
(b)
R = 2
DCEX
CEX
0
1/3
2/3
ρ_{ch}/ρ

Fig. 14